field states occur that provide for rapid nonradiative decay.[21,22b] Consistent with this hypothesis, the emission yield increases in the series $Ru(trpy)_2^{2+} < Ru(trpy)(bpy)(py)^{2+} < Ru(bpy)_3^{2+}$ in line with the anticipated increase in ligand field strength. It should be noted, however, that low-symmetry effects could also be important. Thus, in the case of $Ru(trpy)_2^{2+}$, the dominant low-symmetry component of the ligand field is expected to reflect a tetragonal compression, whereas in the mixed-ligand systems, the low symmetry distortion is more likely to be described in terms of a tetragonal elongation. Unfortunately, the influence that the low-symmetry field has on the energies of the various d–d excited states is difficult to assess even in a qualitative sense.

Conclusions

Ligand reduction, whether achieved via an outer-sphere process or via charge-transfer excitation, tends to be single-ligand-localized in polypyridine complexes. Here the techniques of cyclic voltammetry, spectroelectrochemistry, and EPR spectroscopy have been applied to the problem of discerning the site of electrochemical reduction in mixed-ligand polypyridyl complexes of Ru(II). The results clearly demonstrate that the first reduction in $Ru(trpy)(bpy)(py)^{2+}$, as well as $Ru(trpy)(4,4'\text{-dph-bpy})(py)^{2+}$, is primarily localized on the trpy ligand. Due to the correlation of the emission energies with the electrochemical data, we conclude that the transferred electron density is localized primarily on the trpy ligand in the lowest energy MLCT excited state as well. It seems reasonable that trpy is reduced before bpy because the former presents a more extended π system and presumably more stable π-antibonding orbitals. The 4,4′-dph-bpy ligand may present an even more extended π system; however, there would be considerable steric strain in the fully planar conformation. The presence of an additional nitrogen atom (more electronegative than carbon) in the trpy ligand and a potentially smaller average charge separation in $Ru^{II}(trpy^-)$ versus $Ru^{II}(4,4'\text{-dph-bpy}^-)$ may also favor trpy reduction. Solvation effects may also be important. Finally, the similarities among the g values and the absorption spectra of the singly reduced forms of the mixed-ligand complexes and $Ru(trpy)_2^+$ suggest that localized $trpy^-$ states occur in the latter system as well, in accord with the conclusions of DeArmond and co-workers.[23b]

Acknowledgment. This research was supported by the National Science Foundation through Grant Nos. CHE-8414267 and CHE-8719538. We wish to thank Dr. Jon R. Kirchhoff for his assistance in the fabrication of the OTTLE and for many helpful discussions as well as Phillip M. Hanna for his assistance with the EPR measurements.

Contribution from the Department of Chemistry, College of General Education, Nagoya University, Nagoya 464-01, Japan

XANES Study at the Co K Absorption Edge in a Series of Cobalt(III) Complexes

Mitsuru Sano

Received December 17, 1987

Systematic measurements of Co K-edge spectra have been carried out for a series of cobalt(III) complexes. A counterion effect has been observed in the higher energy region of the XANES. The energy of the 1s–3d transition increased in the following order: $dtc^- < ox^{2-} < NO_2^- <$ phen < NH_3, en < CN^- (dtc^- = diethyldithiocarbamate ion, ox^{2-} = oxalate ion, phen = 1,10-phenanthroline, en = 1,2-diaminoethane). This order is correlated with the energy of the 3d antibonding orbital. One-electron interpretation has been done for $[Co(CN)_6]^{3-}$ and $[Co(NO_2)_6]^{3-}$ spectra with DV–Xα MO calculations and relates the main absorption bands to transitions from the Co 1s orbital to MO's that result from the interaction of the Co 4p and antibonding ligand orbitals. The XANES feature also reflects the symmetry of the complex. Comparisons of XANES spectra have been made between geometrical isomers of $[CoCl_2(en)_2]^+$, $[Co(gly)_3]$ (gly^- = glycinate ion), and $[Co(methio)_2]^+$ ($methio^-$ = methioninate ion).

Introduction

The EXAFS contains structural information on atoms surrounding an X-ray absorbing atom and is now widely used as a powerful tool for structural studies.[1] The analysis of EXAFS is usually made by using parameters whose values may be determined from EXAFS spectra of model compounds or from theoretical considerations. The information derived from EXAFS is only the one-dimensional radial distribution function about an absorbing atom. XANES may give information complementary to that extracted from EXAFS and may reflect the coordination geometry and the electronic structure of the absorbing atom; so this is particularly important in the study of systems for which EXAFS is of limited usefulness. In fact, interests in the determination of the local structure of complex systems like proteins, surfaces, and amorphous materials have renewed attention to XANES.

Although X-ray absorption spectra have been measured for many years,[2] the relations between the intensity, shape, and location of edge features on one hand and the ligand field geometry and electronic structure of the absorbing atom on the other still remain for further systematic studies. Cobalt(III) compounds are suitable for the studies because a wide variety of complexes are easily prepared and are fairly stable.

In the present work, we measured the Co K-edge spectra of a series of cobalt(III) complexes and investigated the relation between the feature of XANES and the nature of the cobalt complex.

Experimental Section

The cobalt(III) complexes except for $K_3[Co(CN)_6]$ were prepared according to standard methods.[3] A small amount of each sample was ground and diluted with boron nitride (ca. 25 mg/140 mg)[4] and contained in a plastic cell between polypropylene windows spaced 1.0 mm apart.

The Co K-edge spectrum was measured by using the EXAFS facilities at Beam Line 10B of the Photon Factory at the National Laboratory for High Energy Physics (KEK-PF). Synchrotron radiation from the electron storage ring (2.5 GeV, average 150 mA) was monochromatized with a channel-cut Si(311) monochromator.[5] The absorption spectrum of a piece of Cu foil was measured simultaneously with acquisition of data on the cobalt complexes, and relative energies were calibrated with respect to the first inflection point of the Cu metal absorption edge, defined to be 8978.8 eV. The incident and transmitted beam intensities were measured with N_2- and Ar(15%)–N_2-filled ionization chambers, respectively. Other instrumental details are given in ref 5. The XANES spectra were obtained from transmission data at room temperature in the

(1) Teo, B. K.; Joy, D. C. *EXAFS Spectroscopy, Techniques, and Applications*; plenum: New York, 1981.
(2) Srivastava, U. C.; Nigam, H. L. *Coord. Chem. Rev.* **1972**, *9*, 275–310.
(3) *Shin-Jikken Kagaku Koza* Maruzen: Tokyo, 1977; Vol. 8.
(4) One of the samples ($[Co(NH_3)_6]Br_3$) was also measured with a different dilution (ca. 12 mg/130 mg), which resulted in no essential difference in the shape of the spectrum
(5) Oyanagi, H.; Matsushita, T.; Ito, M.; Kuroda, H. *KEK Rep.* **1983**, 83-100.

0020-1669/88/1327-4249$01.50/0

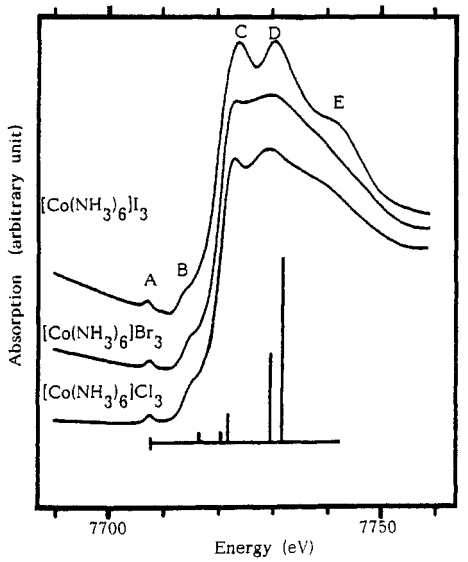

Figure 1. Co K-edge spectra of $[Co(NH_3)_6]X_3$ (X = Cl, Br, and I). The vertical bars show calculated cross-sections for $[Co(NH_3)_6]^{3+}$.

range of photon energy extending from 7680 to 7760 eV. All spectra have been normalized to give an edge jump of 1.0.

Computational Method

The computational details of the DV–Xα MO method have been throughly described by Adachi et al.[6] In the Hartree–Fock–Slater model, the exchange–correlation term is given by

$$-6\alpha[(3/4\pi)\rho(1)]^{1/3}$$

where $\rho(1)$ is the local charge density and α is the exchange-scaling parameter; the value of $\alpha = 0.7$ is used for all atoms throughout the present calculation. The basis sets including the cobalt 1s–5p, Na 1s–3p, C, N, and O 1s–2p, and H 1s orbitals are utilized for the present calculations. The molecular geometries of the complexes are taken from the experimental results.[7-9] In the present calculation, the complexes $[Co(CN)_6]^{3-}$, $[Co(NO_2)_6]^{3-}$, and $[Co(NH_3)_6]^{3+}$ are regarded as having the O_h, D_{2h} (with six equal Co–N distances; corresponding to T_h), and C_s symmetries, respectively.

The oscillator strengths of electric dipole transitions are evaluated by use of

$$f(0\rightarrow j) = (2m\omega_{0j}/3\hbar e^2)|\langle 1s|er|\psi_j\rangle|^2$$

where 1s and ψ_j are the wave functions of the initial orbital (Co 1s) and the final excited orbital, respectively.

Results and Discussion

Counterion Effect. Figure 1 shows the XANES spectra of $[Co(NH_3)_6]X_3$ (X = Cl, Br, and I), which have the same $[Co(NH_3)_6]^{3+}$ chromophore. The spectra are similar to each other except for the higher energy region.

According to ligand field theory, the lowest unoccupied orbital of an octahedral cobalt(III) complex is e_g with metal 3d character, and a weak absorption band associated with quadrupole-allowed or vibronically allowed 1s–3d transitions must appear in the lowest energy region of its XANES. In Figure 1, the small peak A can be related to the 1s–3d transition. Absorption bands B, C, and D also appear in all the spectra given in Figure 1. Band E in the higher energy region is influenced by counterions, suggesting that it orginates not solely from the $[Co(NH_3)_6]^{3+}$ chromophere but from the whole system including counterions. This may be a shape-resonance, in which an electron excited into the continuum state is virtually trapped within the cage (potential barrier) made of the surrounding counter ions.

In order to assign the absorption bands, we carried out the DV–Xα MO calculation for $[Co(NH_3)_6]^{3+}$. The results are compared with the observed spectra in Figure 1. For an easy comparison, the position of the calculated energy of 1s–3d is arbitrarily taken as the reference to be fitted to the corresponding XANES 1s–3d peak in Figure 1. The calculated relative positions and intensities of the transitions show a reasonable correlation with the XANES peaks except for band E, which was not calculated.

As previously discussed, absorption band E can be reasonably assigned to a shape resonance. From comparison with the MO calculation, absorption peaks B and C are assigned to transitions from Co 1s to the NH_3 orbitals and peak D is assigned to the transition to Co p orbitals. Thus XANES spectra will be divided into two regions; one is that of the transitions within the complex ion which can be described by the MO scheme and the other is the higher energy region consisting of a shape resonance that will be easily influenced by the surrounding potentials.

The Fourier transforms of EXAFS for $[Co(NH_3)_6]Cl_3$ and $[Co(NH_3)_6]Br_3$ resembled each other and showed no peaks corresponding to the counterions. This demonstrates that the effect of the distant environment is shown by XANES but not by EXAFS.

Ligand Effect of CoL_6 Complexes. The following discussions are concerned with the XANES spectra of CoL_6-type complexes shown in Figure 2. Although the assignment of the strong absorption bands has not been established in these complexes, the weak absorption peak in the lowest energy region of the XANES spectra should be assigned to the quadrupole-allowed or vibronically allowed 1s–3d transitions.

1s–3d Transition Energy. The 1s–3d transition energies increase in the following order: $[Co(dtc)_3]$ (7706.3 eV) < $K_3[Co(ox)_3]$ (7706.8 eV) < $Na_3[Co(NO_2)_6]$ (7706.9 eV) < $[Co(phen)_3](ClO_4)_3$ (7707.1 eV) < $[Co(NH_3)_6]Cl_3$, $[Co(en)_3]Cl_3$ (7707.3 eV) < $K_3[Co(CN)_6]$ (7708.3 eV) (dtc^- = diethyldithiocarbamate ion, ox^{2-} = oxalate ion, phen = 1,10-phenanthroline, en = 1,2-diaminoethane). This order does not seem to be correlated with their charges. It roughly corresponds to the spectrochemical series[10] ($dtc^- < ox^{2-} < NH_3$, en < phen < $NO_2^- < CN^-$) obtained from their d–d absorption spectra. This can be interpreted as follows. The spectrochemical series is the trend of the energy differences between the dσ and dπ orbitals. Since the overlap integral of the dσ with ligand orbitals is usually larger than that of dπ, the dσ orbital energy is more strongly influenced by the ligands than the dπ orbital energy, and therefore the dσ energy level plays a predominant role in the spectrochemical series, which is the order of Δ (the magnitude of the dσ–dπ splitting). If the energy of the Co 1s orbital remains roughly unchanged in different complexes and the energies of the Co 1s and 3d orbitals are equally affected by counterions, the 1s–3dσ transition energy depends upon the energy level of the unoccupied 3dσ orbital. These arguments lead to a rough correlation between the trend of the 1s–3d transition energy and the spectrochemical series in agreement with experimental findings. This is schematically shown as follows:

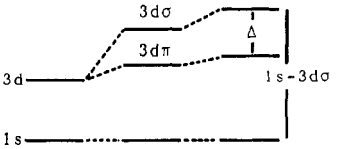

One-Electron Interpretation of the XANES Spectra of $[Co(CN)_6]^{3-}$ and $[Co(NO_2)_6]^{3-}$. Multiple-scattering calculations were made for investigating the XANES of $[Fe(CN)_6]^{4-}$ and $[Fe(CN)_6]^{3-}$ by Bianconi et al.[11] Although they were successful in interpreting the XANES features, no correlation was shown of each peak with a resulting electronic state. Kosugi et al.[12] suc-

(6) Adachi, H.; Shiokawa, S.; Tsukada, M.; Satoko, C.; Sugano, S. *J. Phys. Soc. Jpn.* **1978**, *45*, 875–883.
(7) Vannerberg, N. G. *Acta Chem. Scand* **1972**, *26*, 2863–2876.
(8) Ohba, S.; Toriumi, K.; Saito, Y. *Acta Crystallogr.* **1978**, *B34*, 3535–3542.
(9) Iwata, M.; Saito, Y. *Acta Crystallogr.* **1973**, *B29*, 822–832.
(10) Figgis, B. N. *Introduction to Ligand Fields*; Wiley: New York, 1966.
(11) Bianconi, A.; Dell'Ariccia, M.; Durham, P. J.; Pendry, J. B. *Phys. Rev. B: Condens. Matter* **1982**, *B26*, 6502–6508.
(12) Kosugi, N.; Yokoyama, T.; Asakura, K.; Kuroda, H. *Chem. Phys.* **1984**, *91*, 249–256.

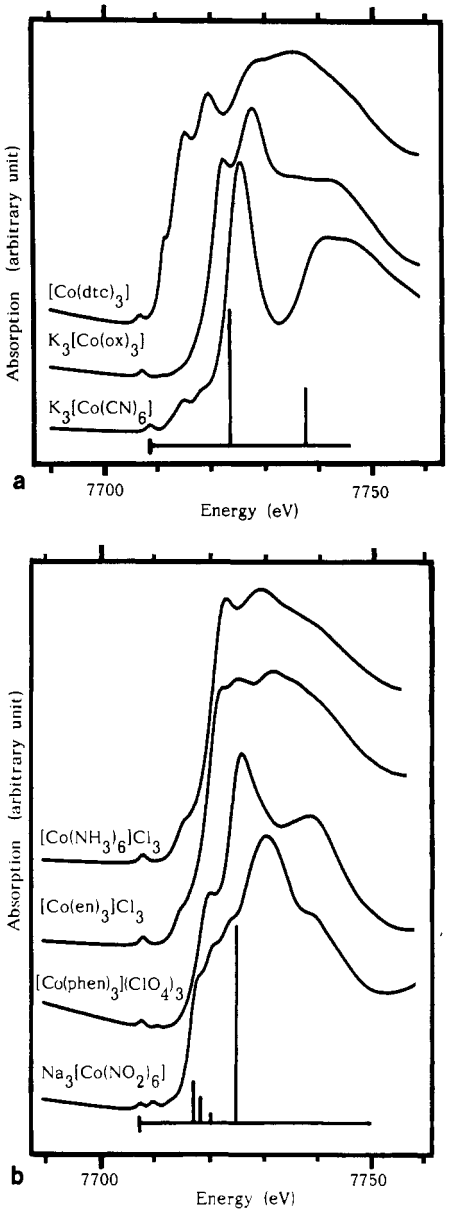

Figure 2. Co K-edge spectra: (a) for Co(III) complexes, with vertical bars showing calculated cross sections for $[Co(CN)_6]^{3-}$; (b) for CoN_6 complexes, with vertical bars showing calculated cross sections for $[Co(NO_2)_6]Na_{14}^{11+}$.

Table I. Molecular Orbital Calculations for $[Co(CN)_6]^{3-}$

symmetry	orbital energy, eV	oscillator strength	symmetry	orbital energy, eV	oscillator strength
$1a_{1g}$	−7499.05		$10t_{1u}$	21.81	0.006 80
$6e_g$	6.57		$11t_{1u}$	27.74	0.000 02
$9t_{1u}$	10.28	0.000 03	$12t_{1u}$	35.88	0.002 89

cessfully explained some peaks of XANES by means of molecular orbital calculation. In the present paper, molecular orbital calculations were made for $K_3[Co(CN)_6]$ and $Na_3[Co(NO_2)_6]$ in order to obtain energies of electronic excitation of the complexes and correlate them with the peaks of XANES. The experimental and calculated transition energies are compared in Figure 2a,b, in which the energy of the 1s–3d transition is taken as the reference in the comparison of the calculated energies with the XANES spectra. Numerical results including electric dipole transition moments are given in Tables I and II. The calculated patterns generally correspond to the observed absorption bands except for the shoulder in the higher energy region.

We shall first consider the XANES of $[Co(CN)_6]^{3-}$. Since $[Co(CN)_6]^{3-}$ has O_h symmetry, electric dipole allowed transitions will occur between the 1s and the t_{1u} MO's. The contours of

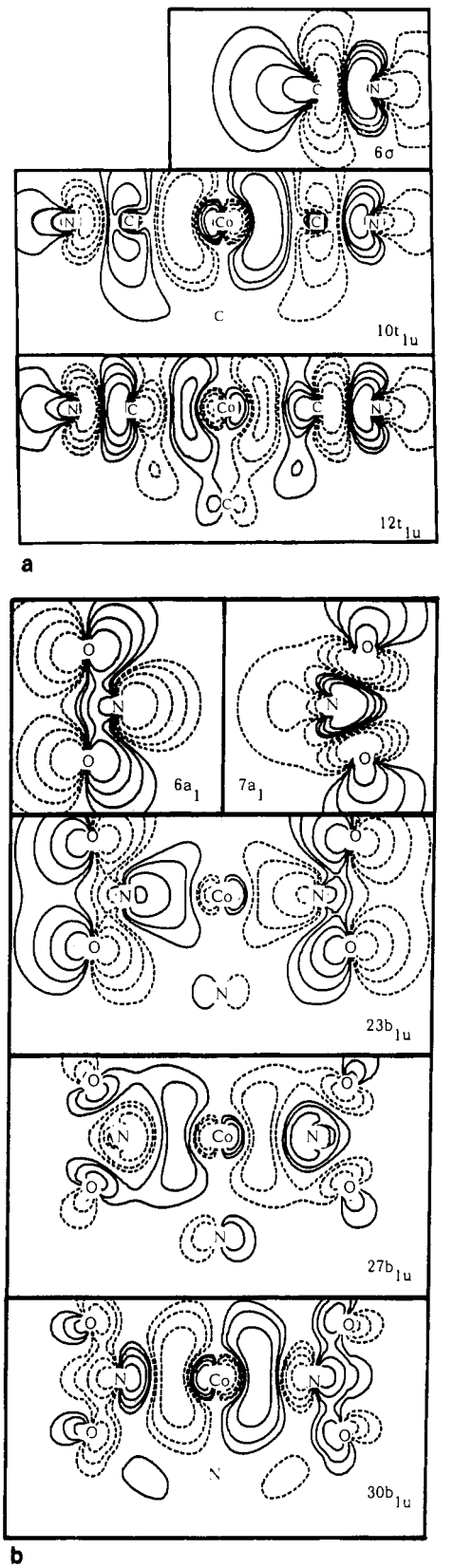

Figure 3. Selected wave-function contours: (a) for $10t_{1u}$ and $12t_{1u}$ orbitals of $[Co(CN)_6]^{3-}$ and the 6σ orbital of CN^-; (b) for 23 b_{1u}, $27b_{1u}$, and $30b_{1u}$ orbitals of $[Co(NO_2)_6]Na_{14}^{11+}$ and $6a_1$ and $7a_1$ orbitals of NO_2^-.

unoccupied t_{1u}-type MO's of $[Co(CN)_6]^{3-}$ given in Figure 3a show that the vacant t_{1u}-type orbitals are composed of Co p and CN^- 6σ orbitals. The transition probability increases with increasing contribution of Co p orbitals to the t_{1u} MO's. As seen from the figure, the CN^- 6σ orbital has its lobe extending toward the cobalt atom and largely overlaps with the Co orbitals. The energy of

Table II. Molecular Orbital Calculations for $[Co(NO_2)_6]Na_{14}^{11+}$

symmetry	orbital energy, eV	oscillator strength	symmetry	orbital energy, eV	oscillator strength
$1a_{1g}$	−7541.98		$27b_{1u}$	−24.91	0.000 42
$36a_{1g}$	−34.65		$27b_{3u}$	−24.80	0.000 23
$37a_{1g}$	−34.48		$27b_{2u}$	−24.12	0.000 48
$24b_{2u}$	−34.41	0.000 02	$28b_{3u}$	−23.40	0.000 55
$24b_{1u}$	−34.23	0.000 02	$28b_{1u}$	−23.17	0.000 02
$24b_{3u}$	−33.97	0.000 02	$28b_{2u}$	−22.92	0.000 20
$25b_{2u}$	−27.88	0.000 00	$29b_{2u}$	−21.63	0.000 03
$25b_{3u}$	−27.82	0.000 00	$29b_{1u}$	−21.34	0.000 11
$25b_{1u}$	−27.81	0.000 00	$29b_{3u}$	−20.80	0.000 10
$26b_{1u}$	−26.25	0.000 00	$30b_{2u}$	−17.82	0.001 44
$26b_{3u}$	−26.02	0.000 00	$30b_{1u}$	−16.79	0.001 68
$26b_{2u}$	−26.01	0.000 00	$30b_{3u}$	−16.70	0.002 15

the Co 4p orbital is nearly the same as that of the CN^- 6σ orbital. They interact with each other to result in two MO's, $10t_{1u}$ and $12t_{1u}$, which are 4p + 6σ and 4p − 6σ, respectively.

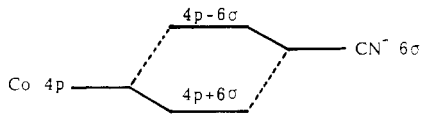

The extent of this mixing determines the intensity of the electric dipole transition. Other unoccupied t_{1u} molecular orbitals have CN^- 2π as the main component, and transitions to these orbitals will be associated with a weak absorption. The XANES of $K_3[Co(CN)_6]$ shows two strong absorption bands and a shoulder in the higher energy region. One of the strong absorption bands can be related to the transition from Co 1s to the 4p + 6σ MO with a large contribution from the Co 4p orbital. The other may be attributed to a transition to an antibonding MO possibly composed of Co 4p, Co 5p, and antibonding σ orbitals of the CN^- ligands. Two small absorption bands at 7714 and 7718 eV and a shoulder in the higher energy region are assigned to transitions of different types. The energy of the shoulder, about 7747 eV, is near that in $[Co(NH_3)_6]^{3+}$, which is influenced by counterions as described above. This suggests that the shoulder can be assigned to the shape resonance.

The feature of the XANES of $Na_3[Co(NO_2)_6]$ is more complicated than that of $K_3[Co(CN)_6]$. Since $[Co(NO_2)_6]^{3-}$ has D_{2h} symmetry, three cobalt 4p orbitals are classified into b_{1u}, b_{2u}, and b_{3u} orbitals and interact with symmetry orbitals of the ligands. The interacting orbitals are Co 4p, NO_2^- σ-type orbitals ($6a_1$ and $7a_1$) and π-type orbitals (one perpendicular to the molecular plane of NO_2^- and the other in plane). The resulting MO's then have different degrees of contribution from the Co 4p orbital, leading finally to the complicated XANES of $[Co(NO_2)_6]^{3-}$. In order to discuss the XANES for $[Co(NO_2)_6]^{3-}$, DV-Xα MO calculations of two clusters, $[Co(NO_2)_6]^{3-}$ and $[Co(NO_2)_6]Na_{14}^{11+}$ were made. (The calculation of $[Co(NO_2)_6]Na_{14}^{11+}$ includes $[Co(NO_2)_6]^{3-}$ and its counterions, which are distributed according to the three-dimensional structure.[8]) The two calculations gave almost the same results. Since both clusters have D_{2h} symmetry, dipole-allowed transitions occur between the Co 1s orbital to b_{1u}, b_{2u}, and b_{3u} MO's (which correspond to the t_u MO in T_h symmetry). In order to assign absorptions, the contours of b_{1u} MO's with a considerable contribution of Co p are given in Figure 3b, which also shows contours of the NO_2^- $6a_1$ and $7a_1$ orbitals. As seen from Figure 3b, the 27 b_{1u} MO is constituted of the Co 4p orbital and the $7a_1$ orbitals of NO_2^- with larger contribution from the ligand orbitals. The 30 b_{1u} MO consists of the Co 4p (possibly mixed with 5p) and NO_2^- $6a_1$ orbitals. The b_{1u} MO's that are related to XANES can be illustrated as follows.

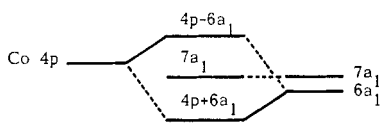

The order of orbital energies is $6a_1 < 7a_1 <$ Co 4p. The $7a_1$ orbital scarcely interacts with Co 4p owing to its low population near the Co atom. On the other hand, the $6a_1$ MO strongly interacts with the Co 4p orbital to result in two MO's, $6a_1$ + 4p and 4p − $6a_1$. The $30b_{1u}$ MO, 4p − $6a_1$, has a large contribution of the Co 4p orbital and can be related to the intense band appearing at 7730 eV of the spectrum of $Na_3[Co(NO_2)_6]$. The 28 b_{1u} and $29b_{1u}$ MO's are mainly composed of the antibonding b_1 and b_2 orbitals of NO_2^-, and the small intensities are attributable to a slight π-type mixing with the Co 4p orbital, so that they may be related to shoulders of low intensity. The shoulder in the higher energy region, however, cannot be interpreted by MO calculations and should be considered to be the shape resonance.

The shakedown transitions with strong absorption that are usually found in divalent transition-metal complexes[12,13] were not

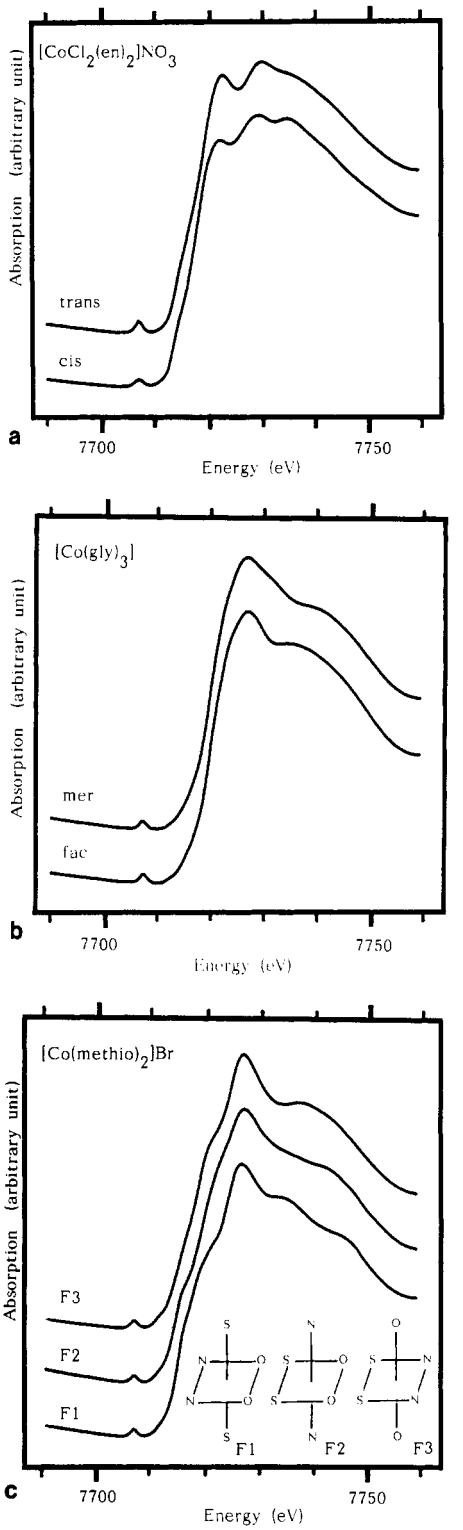

Figure 4. Co K-edge spectra: (a) for *cis*- and *trans*-$[CoCl_2(en)_2]NO_3$; (b) for *mer*- and *fac*-$[Co(gly)_3]$; (c) for the F_1, F_2, and F_3 isomers of $[Co(methio)_2]Br$.

observed in these cobalt(III) complexes. This is consistent with the fact that the 2p peaks in the X-ray photoelectron spectra of cobalt(III) complexes are rarely accompanied by shake-up satellite peaks.[14]

Comparison of CoL_6 Spectra. No common characteristic features of the XANES spectra are found for CoL_6 complexes, except that the main absorption peaks are found around 7730 eV for all the complexes examined. According to the MO calculations, these absorption bands are assigned to the transition from Co 1s orbital to an MO with a Co p orbital as a main component. This means that the 1s–4p orbital energy difference remains almost the same for all the trivalent cobalt complexes examined.

Absorption in the range from the 1s–3d to the 1s–4p transition significantly changes among these complexes. Several intense absorption bands near the edge are found for $[Co(dtc)_3]$ but not for $K_3[Co(CN)_6]$. The dtc ligand has unoccupied MO's to be mixed with the Co 4p orbital. On the other hand, the CN^- ligand has only one unoccupied orbital, 6σ, which can strongly interact with the Co 4p orbital. The absorption near the edge is correlated with unoccupied orbitals of the ligand in cobalt complexes. These suggest that the nature of the ligands reflects on the absorptions before the main peaks.

Isomer Effect. In order to study the relationship between the XANES spectrum and the symmetry around the cobalt ion, the XANES spectra for *cis*- and *trans*-$[CoCl_2(en)_2]NO_3$ (en = 1,2-diaminoethane), for *mer*- and *fac*-$[Co(gly)_3]$ (gly = glycinate ion), and for the F_1, F_2 and F_3 isomers of $[Co(methio)_2]Br$ (methio = L-methionate ion) are compared in Figure 4a–c. The general features of the XANES spectra are similar between isomers.

Spectra of *cis*- and *trans*-$[CoCl_2(en)_2]NO_3$ show differences in the shoulder on the higher energy side; for the trans complex, the shoulder is so pronounced as to become a third peak. On the other hand, the 1s–3d peak is higher for the cis than for the trans complex in agreement with the group-theoretical consideration that this transition is less strictly forbidden in the cis complex with a lower symmetry of C_{2v} as compared with the quasi-D_{2h} symmetry of the trans complex.

Figure 4c shows the XANES spectra of $[Co(methio)_2]Br$ isomers in which methioninate ions are coordinated with the cobalt ion at sulfur, oxygen, and nitrogen atoms. The spectra show differences at the high-energy side of the main peak; isomer F_1, which has two S atoms at trans positions to each other, has a spectrum with two peaks at the high-energy shoulder, whereas the spectra of F_2 and F_3, which have the S atoms at cis positions, show one broad peak at the shoulder. The spectral features of the isomers are parallel to those of $[CoCl_2(en)_2]NO_3$ isomers, considering that O and N as ligators are located near to each other in the spectrochemical series but S is far apart from them.

These examples show that XANES spectra reflect, though not always sensitively, the structure around the absorbing atom.

Conclusions

A systematic study of XANES spectra has been carried out for a series of cobalt(III) complexes. This led to the following conclusions.

(1) The counterion effect has been observed in the XANES spectra of $[Co(NH_3)_6]X_3$ (X = Cl, Br, and I) in their higher energy region, demonstrating that the XANES spectra can exhibit the effect of distant environment which EXAFS cannot show.

(2) The trend of the 1s–3d transition energies is $dtc^- < ox^{2-} < NO_2^- <$ phen $< NH_3$, en $< CN^-$, which roughly corresponds to the spectrochemical series.

(3) According to MO calculations for $[Co(CN)_6]^{3-}$ and $[Co(NO_2)_6]^{3-}$, the main absorption bands can be interpreted as transitions from Co 1s to MO's resulting from the interaction of Co 4p with ligand σ antibonding orbitals.

(4) The general features of XANES spectra differ only slightly between geometrical isomers; however, the XANES spectra appreciably differ between isomers when coordinating atoms considerably differ in their spectrochemical properties.

(5) These findings show that XANES contains very important information on the electronic and geometrical structures around the absorbing atom. Further systematic studies of XANES spectra on series of complexes will establish a general rule.

Acknowledgment. I thank Prof. Hideo Yamatera for his useful discussion and his encouragement. I also thank Prof. Hirohiko Adachi for his advice on the molecular orbital calculations. This work has been performed under the approval of the Photon Factory Program Advisory Committee (Proposal No. 86015).

(13) Bair, R. A.; Goddard, W. A., III. *Phys. Rev. B: Condens. Matter* **1980**, *22*, 2767–2776.
(14) Frost, D. C.; McDowell, C. A.; Woolsey, I. S. *Mol. Phys.* **1974**, *27*, 1473–1489.

Contribution from the Department of Chemistry, The University of Calgary, Calgary, Alberta, Canada T2N 1N4

Silicon-29 NMR Studies of Aqueous Silicate Solutions. 1. Chemical Shifts and Equilibria

Stephen D. Kinrade† and Thomas W. Swaddle*

Received November 25, 1987

In the ^{29}Si NMR spectra of aqueous alkali-metal (M) silicate solutions ($[MOH]:[Si^{IV}] = 1.0$ or higher), variations in solution composition cause displacements of the peaks of up to 1 ppm, largely through interaction of silicate units with M^+. The analysis of the chemical shift data provides a means of predicting ^{29}Si resonance frequencies for new silicate species and has aided in the identification of the $Si_4O_{10}^{4-}$ (Q^3_4) anion, in which the Si atoms are at the corners of a regular tetrahedron. A quantitative study of the dependence of silicate connectivity upon temperature (−5 to +144 °C) and solution composition shows that silicate polymerization is favored by low temperature, low alkalinity, and high $[Si^{IV}]$. In no case could silicate centers with 4-fold connectivity (Q^4) be detected. The effect of M^+ on the distributions of silicate species is small, but the larger M^+ atoms do preferentially stabilize the more highly polymerized silicate anions.

Introduction

The characterization ("speciation") of dissolved silicates in aqueous fluids has long presented a major problem in various geological and technological contexts. Potentiometric studies, in which pH values rather than actual silicate concentrations were measured, have shown that polymerization of aqueous silicates is important and is favored by low temperatures, high Si concentration, and low alkalinity.[1] Raman spectra of aqueous silicate solutions are not very well-defined but suggest that the observed distribution of silicate species is independent of both the solution

†Present address: Department of Chemistry, Lakehead University, Thunder Bay, Ontario, Canada P7B 5E1.

(1) Busey, R. H.; Mesmer, R. E. *Inorg. Chem.* **1977**, *16*, 2444.

0020-1669/88/1327-4253$01.50/0